The Use of External Transducers for Estimating Bone Strain at the Distal Tibia During Impact Activity

W. Brent Edwards[1]
Department of Kinesiology,
Iowa State University,
Ames, IA 50011
e-mail: edwards9@iastate.edu

Erin D. Ward
Central Iowa Foot Clinic,
Perry, IA 50220

Stacey A. Meardon

Timothy R. Derrick

Department of Kinesiology,
Iowa State University,
Ames, IA 50011

*Noninvasive methods for monitoring the in vivo loading environment of human bone are needed to determine osteogenic loading patterns that reduce the potential for bone injury. The purpose of this study was to determine whether the vertical ground reaction impact force (impact force) and leg acceleration could be used to estimate internal bone strain at the distal tibia during impact activity. Impact loading was delivered to the heels of human-cadaveric lower extremities. The effects of impact mass and contact velocity on peak bone strain, impact force, leg acceleration, and computed impact force (leg acceleration*impact mass) were investigated. Regression analysis was used to predict bone strain from six different models. Apart from leg acceleration, all variables responded to impact loading similarly. Increasing impact mass resulted in increased bone strain, impact force, and computed impact force, but decreased leg acceleration. The best models for bone strain prediction included impact force and tibial cross-sectional area ($R^2=0.94$), computed impact force and tibial cross-sectional area ($R^2=0.84$), and leg acceleration and tibial cross-sectional area ($R^2=0.73$). Results demonstrate that when attempting to estimate bone strain from external transducers some measure of bone strength must be considered. Although it is not recommended that the prediction equations developed in this study be used to predict bone strain in vivo, the strong relationship between bone strain, impact force, and computed impact force suggested that force platforms and leg accelerometers can be used for a surrogate measure of bone strain.*
[DOI: 10.1115/1.3118762]

Keywords: bone loading, impact force, acceleration, effective mass

1 Background

The foot-ground contact that occurs during locomotion and impact activity results in an impact force that gets transmitted up the musculoskeletal system. Although the muscles of the lower extremity may attenuate some of the impact force [1], a portion is absorbed via bone deformation (i.e., bone strain). Bone strain, or some consequence thereof, plays an important role in bone adaptation [2–4]. Numerous studies have observed greater bone mass in athletes participating in high impact sports [5–7]. In addition, athletes participating in high impact sports have the greatest prevalence of stress fracture [8,9]. The ability to quantify bone strain in vivo may help to better elucidate loading patterns that maximize the osteogenic response and minimize the potential for bone injury.

Indeed, bone strain can be monitored in vivo with the use of strain gauges applied to the bone surface [10–12]. However, the direct measurement of bone strain requires invasive surgical procedures, and human subject review boards are hesitant to grant approval of such techniques in the United States. For this reason, it is common practice to use external transducers, such as force platforms and accelerometers, for an indirect or surrogate measure of bone strain [13].

The vertical ground reaction impact force (impact force) is one of the most widely used parameters to quantify impact loading [14–16]. However, two people receiving similar impact forces may experience dissimilar bone strains. For a given load, the determinants of bone strain are dependent on bone size, shape, and material properties. Accounting for all of these variables may be impractical or even unnecessary in a clinical setting, but bone cross-sectional area can be obtained with great precision and relative ease using computerized tomography [17]. As both force and area determine bone stress in an axial loading scenario, inclusion of bone cross-sectional area may improve the estimation of bone strain when impact force is used as a surrogate measure.

Similar considerations about bone strain determinants must be taken into account when attempting to estimate internal bone strain from accelerometry. During impact assessment, accelerometers are typically mounted to the distal leg because the limited amount of soft-tissue at this location provides a more realistic measure of bone loading [18]. In addition, the distal tibia is a common location for stress fracture [8,9], and researchers have used accelerometers at this site to investigate risk factors for stress fracture development [19–21]. An important consideration is that the measurement of impact acceleration is sensitive to changes in the body's effective mass during impact. Changes in effective mass may result as a function of lower leg geometry at contact [22]. Although a larger effective mass will lead to an increase in impact force, this mass is harder to accelerate, and does not necessarily lead to an increase in impact acceleration [23]. In this instance it is necessary to multiply impact acceleration by effective mass, so that the force of the impact can be approximated.

Force platforms and accelerometers provide a practical means with which to assess bone loading as they are noninvasive and inexpensive to use. However, the relationship between parameters measured with these devices and internal bone stain remains unclear. The purpose of this study was to determine whether the

[1]Corresponding author.

Contributed by the Bioengineering Division of ASME for Publication in the Journal of Biomechanical Engineering. Manuscript received July 19, 2007; final manuscript received January 2, 2009; published online April 14, 2009. Review conducted by Avinash Patwardhan.

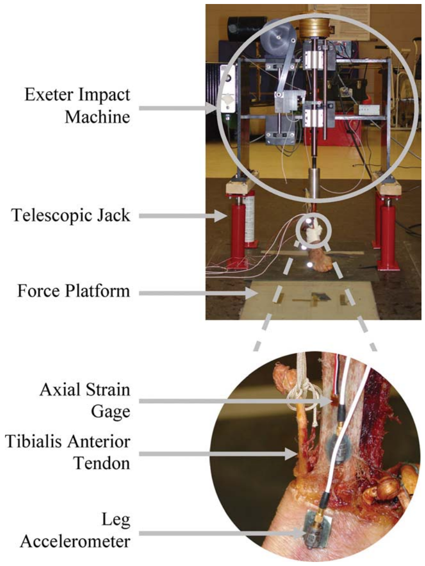

Fig. 1 Impact tester and instrumentation

impact force and leg acceleration could be used to estimate internal bone strain at the distal tibia during impact activity. It was hypothesized that the impact force, in combination with bone cross-sectional area, would be a strong predictor of bone strain. It was also hypothesized that leg acceleration, in combination with bone cross-sectional area, would be a strong predictor of bone strain after accounting for changes in impact mass.

2 Method of Approach

2.1 Specimens. Five human frozen lower extremities with tibia/fibula osteotomy 20 cm above the malleoli were obtained from five separate medical cadavers (age range within 32–80 years). All lower limbs were from the right leg and of mixed death histories. Only cadaveric specimens free from structural pathologies, as identified by a podiatrist, were included in the study. Skin and soft tissue 4 cm above the malleoli were removed for access to tendons crossing the ankle (Fig. 1). The tibial periosteum was removed and the bone surface was prepared in accordance with Vishay Measurements Group Application Note B-1290–8.

A rectangular rosette strain gauge (CEA-06–062UW-350, Vishay Micro-Measurements, Raleigh, NC) was mounted to the distal anteriomedial tibia of one of the cadaveric specimens. However, the strain located along the transverse plane of the bone was negligible, and an anisotropic stress analysis [24] revealed that our testing regimen imposed primarily longitudinal loading. Therefore, a uni-axial strain gauge (CEA-06–06UW-350, Vishay Micro-Measurements, Raleigh, NC) was mounted in-line with the longitudinal axis of the bone for the remaining four cadaveric specimens. The longitudinal axis was defined by a line connecting the ankle joint center to the centroid location of the tibial cross section at the site of osteotomy. The gauge was bonded to the anteriomedial tibial shaft 10 cm above the medial malleolus. In addition, a uni-axial piezoelectric accelerometer (Model 353B, PCB Piezoelectronics, Depew, NY) was mounted to the skin of the distal anteriomedial face of the leg. The accelerometer was embedded in petro wax (PCB Piezoelectronics, Depew, NY), fixed to a hard plastic backing, and adhered to the remaining soft tissue 2–3 cm above the medial malleolus using cyanoacrylate glue (Fig. 1). Proflex elastic athletic tape was then wrapped around the leg to minimize skin movement artifact. Finally, retroreflective markers were placed on the heel and fifth metatarsal of the cadaveric extremities in order to quantify foot angle at contact.

2.2 Data Collection. An Exeter impact testing system (Exeter Research, Inc., Exeter, NH) was situated over a force platform (AMTI, Watertown, MA) and used to deliver impact loading to the heel of each foot (Fig. 1). The factory load cell was removed, and a 3/8 in. aluminum rod was used to connect the proximal end of the tibia to a custom made missile head at the distal end of the impacting shaft. The rod was driven into the intramedullary canal of the tibia and fixated with two bolts. The distal end of the rod was approximately 5 cm above the strain gauge location. Foot angle was controlled prior to impact by applying tension to the anterior tibialis tendon. A digital force transducer revealed that 24.4 ± 3.1 N of tension was applied to the tendon. The tendon was tied to a braided Kevlar line and connected to surgical tubing that was attached to the missile head of the impact testing system. The surgical tubing allowed for foot flexion prior to impact, and the commencement of foot extension upon impact.

Each cadaveric extremity was dropped six times in each of four conditions, consisting of two drop heights and two masses. Drop heights of 3 cm and 5 cm were used to simulate contact velocities approximating -0.80 m/s and -1.0 m/s, respectively. These values fall within the range of contact velocities reported for human walking and running (0.4–1.5 m/s) [25]. Masses of 9 kg and 11 kg were chosen to elicit physiologically relevant changes in effective mass typically seen during human locomotion and impact activity (5–11 kg) [22]. Mass was manipulated with calibrated plates attached to the proximal end of the impacting shaft. Due to small differences in cadaveric specimen masses, the average impact mass was 8.77 ± 0.18 kg and 10.77 ± 0.18 kg for the 9 kg and 11 kg conditions, respectively.

2.3 Data Analysis. Strain gauge, accelerometer, force platform, and motion capture data were collected concurrently with an eight-camera Peak Motus 3D optical capture system (Vicon Peak, Centennial, CO). Analog data were collected at 3600 Hz and motion capture data at 120 Hz. Smoothing procedures were implemented using a fourth order zero-lag Butterworth filter. Motion capture data were filtered with a low-pass cutoff frequency of 6 Hz. Resonant frequency components of a skin mounted accelerometer range between 60–100 Hz, while the true impact frequencies occur below 50 Hz [26]. If the raw acceleration signals are analyzed in the time domain the degree of amplification due to the attachment can range between 8% and 23% [27,28]. For this reason accelerometer data were filtered with a low-pass cutoff frequency of 60 Hz. The strain signal was not free from noise and therefore was filtered with a low-pass cutoff frequency of 80 Hz. A source of error may have been from electrical noise caused by strain gauge wire movement during impact. A cumulative power spectral analysis revealed that a cutoff frequency of 80 Hz maintained 95% of the raw signal and the resulting attenuation of peaks in the time domain was less than 10%. A post-hoc sensitivity analysis comparing the filtered to the raw signal revealed that the cutoff frequency did not change the significance or interpretation of the results.

Foot angle upon impact, foot range of motion, and peak magnitudes of strain, acceleration, and impact force were calculated. Only the gauge element in-line with the longitudinal axis of the bone was analyzed for the cadaveric specimen with the rectangular rosette. In addition, the leg acceleration was multiplied by the impact mass to obtain "computed impact force," an approximation of impact force. The accelerometer measures 0 g when acted on by earth's gravity. Therefore, 1 g was added to the peak leg acceleration before converting to m/s^2 and multiplying by impact mass to obtain the computed impact force measurement in newtons.

Following impact testing, cross-sectional area was obtained for each tibia. A small cross section, approximating 1.5 cm in length that included the strain gauge mounting site, was removed from the bone. A digital photo of the cross section was captured, and the cross-sectional area was calculated by summing bone pixels of a scaled thresholded image.

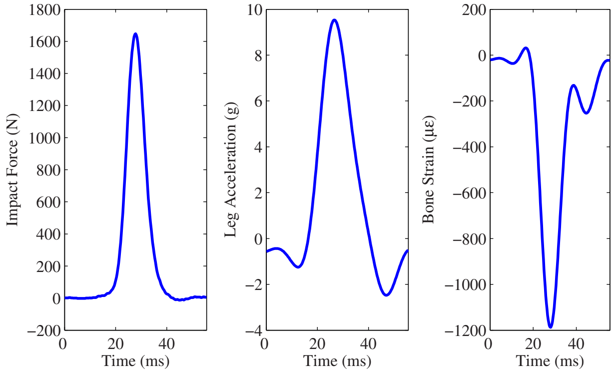

Fig. 2 Typical impact force, leg acceleration, and bone strain profiles during impact. The bone strain profile has a negative value indicating a compressive strain.

2.4 Statistics. A 2×2 factor repeated measures analysis of variance (ANOVA) was used to examine the effects of impact mass and contact velocity on peak bone strain, impact force, leg acceleration, and computed impact force. Simple and multiple regressions were used to predict bone strain from six different models. The predictor variables in these models included: (a) impact force; (b) impact force and cross-sectional area, (c) leg acceleration, (d) leg acceleration and cross-sectional area, (e) computed impact force, and (f) computed impact force and cross-sectional area. Prior to statistical analysis, trials were collapsed across conditions. Statistical analysis was performed in JMP 5.1 with a criterion alpha level of 0.05.

3 Results

The impact loading device produced similar impact profiles for impact force, leg acceleration, and bone strain (Fig. 2). Peak impact occurred at approximately 8–15 ms following heel contact. On average the foot was approximately 6 deg flexed at contact, and went through a range of motion of approximately 6 deg after contact.

The ANOVA results showed a significant main effect for contact velocity and impact mass for each dependent variable (Table 1). No interactions were observed. Peak impact force behaved similar to peak bone strain during impacts. Increased contact velocity and impact mass caused both the impact force and bone strain to increase. Peak leg acceleration also behaved similar to peak bone strain and impact force with increased contact velocity; however, increased impact mass caused peak leg acceleration to decrease. This was an anticipated relationship that was corrected by multiplying leg acceleration by the impact mass. The resulting computed impact force increased during 11 kg conditions, similar to bone strain and impact force.

The thresholding procedure used to calculate tibial cross-sectional area resulted in an image resolution ranging between 0.0267 mm/pixel and 0.0283 mm/pixel. Cross-sectional areas ranged from 1.62 cm^2 to 2.44 cm^2, with an average of 1.97 cm^2 (Table 2).

Table 2 Tibial cross-sectional area (CSA) for five cadaveric specimens. Tibial location was approximately 10 cm above the medial malleolus.

	Foot 1	Foot 2	Foot 3	Foot 4	Foot 5
CSA (cm^2)	1.62	1.78	2.44	1.99	2.03

Inclusion of cross-sectional area into the regression models for impact force, leg acceleration, and computed impact force improved the coefficients of determination (Fig. 3 and Table 3). Of the three models, including cross-sectional area, impact force had the best prediction of bone strain (Table 3, $R^2=0.94$, and RMSE $=98\ \mu\varepsilon$) and leg acceleration had the worst prediction of bone strain (Table 3, $R^2=0.73$, and RMSE$=214\ \mu\varepsilon$).

4 Discussion

The purpose of this study was to determine whether the impact force and leg acceleration could be used to estimate internal bone strain at the distal tibia. Cadaveric simulation was a practical method to examine this relationship because it allowed for the measurement of bone strain with controlled manipulation of contact velocity and impact mass. Both hypotheses were supported by the results of this study. The impact force and leg acceleration accounted for a relatively small percentage of variance in bone strain (62% and 38%, respectively). However, when combined with tibial cross-sectional area, the impact force became a strong predictor of internal bone strain (94%). After accounting for impact mass, a similar result was found for leg acceleration (84%).

For each foot, increasing the contact velocity and impact mass resulted in a larger compressive strain. With respect to changes in velocity, both the impact force and leg acceleration behaved similarly to bone strain. Increasing the contact velocity resulted in an increase in impact force and a parallel increase in leg acceleration. Increasing mass increased the impact force, but caused the leg acceleration to decrease. To adjust for this discrepancy, the leg acceleration was multiplied by the impact mass to obtain computed impact force. Computed impact force increased during the 11 kg conditions, similar to bone strain and impact force.

The effective mass during this study was essentially the mass of our entire system. This is contrary to normal human impact activity in which the effective mass is only a portion of the entire body mass. In humans, the decoupling and rotation of lower extremity segments during landing determine the mass contribution, or effective mass, during impact [23]. Using a combination of modeling results and experimental data for walking, running, and jumping, Denoth [22] estimated the effective mass as a function of knee contact angle. For a 65 kg subject, changing knee flexion from 5 deg to 20 deg at impact resulted in an effective mass change from 11 kg to 5 kg. As such, the impact masses of 9 kg

Table 1 Group means (1SD) for peak bone strain, impact force, leg acceleration, and computed impact force. All main effects of contact velocity and impact mass were significant.

Contact velocity (m/s)	Impact mass (kg)	Bone strain ($\mu\varepsilon$)	Impact force (N)	Leg acceleration (g)	Computed impact force (N)
−0.80	9	527 (264)	855 (360)	5.7(2.4)	573 (207)
	11	716 (380)	1028 (454)	5.3(2.5)	664 (258)
−1.00	9	719 (338)	1195 (456)	7.8(2.8)	752 (239)
	11	941 (439)	1371 (544)	6.9(2.9)	835 (302)
Main effect of velocity (p-value)		0.01	>0.01	>0.01	>0.01
Main effect of mass (p-value)		0.02	0.02	>0.01	0.04

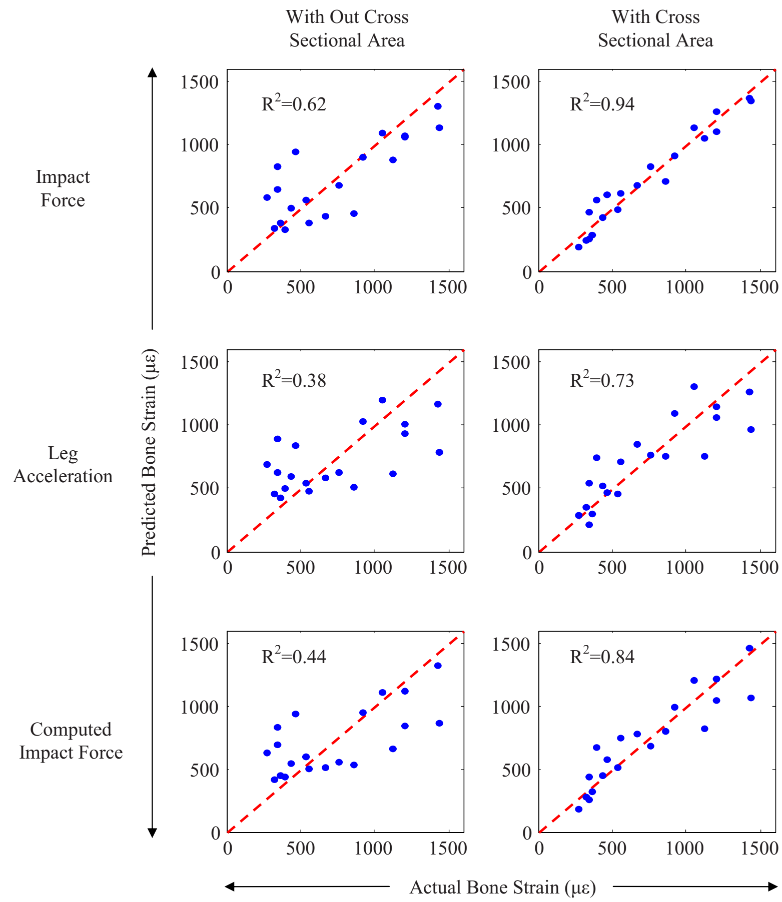

Fig. 3 Actual bone strain versus predicted bone strain for the six regression models. The dashed line at 45 deg represents a theoretical line of perfect prediction.

and 11 kg used during this study have direct implications for researchers wanting to use leg acceleration as a means to quantify impact magnitude. When making comparisons between conditions in which even small changes in lower leg geometry may occur during contact, the effective mass of the impact or some related measure must be taken into account. For this reason, future research should look to establish a reliable means with which to experimentally assess effective mass.

The method by which effective mass was manipulated in this study warrants further discussion. A considerable amount of soft-tissue proximal to the ankle was removed for access to extrinsic tendons crossing the joint. This mass was replaced with weights approximating the effective mass of the leg during impact. Although it is possible that this mass could have resulted in a different magnitude of acceleration compared with the soft tissue, our values are in agreement with previous literature. An in vivo study by Mercer et al. [29] measured peak leg accelerations ranging from 6.1 g to 10.9 g during running. Peak acceleration magnitudes for our simulated running conditions (contact velocity −1.0 m/s) ranged from 6.9 g to 7.8 g. Consequently, we feel that our manipulation of effective mass was acceptable.

As evidenced in this study, the estimation of internal bone loading from external transducers can be improved if the cross-sectional area is considered. Of the six regression models used for statistical analysis, the three models including tibial cross-sectional area had the lowest prediction error. In each case, the beta coefficients for cross-sectional area were negative. This would indicate that a larger cross-sectional area resulted in a decrease in bone strain. Cross-sectional area was used in this study because it was assumed that the tibial compression was primarily due to axial loading during impact. When tibial bending is the primary mode of mechanical loading, it may be better to include

Table 3 Beta coefficients, coefficient of determination, and root mean squared error for the six regression models

Model	β_0	β_1	β_2	R^2	RMSE ($\mu\varepsilon$)
a	Intercept 47	Impact force (N) 0.61		0.62	249
b	Intercept 1538	Impact force (N) 0.69	Cross-sectional area (cm^2) −802.07	0.94	98
c	Intercept 186	Leg acceleration (g) 84.80		0.38	317
d	Intercept 1718	Leg acceleration (g) 105.81	Cross-sectional area (cm^2) −845.39	0.73	214
e	Intercept 60	Computed impact force (N) 0.95		0.44	301
f	Intercept 1658	Computed impact force (N) 1.20	Cross-sectional area (cm^2) −902.49	0.84	167

area moment of inertia. Including some measure of bone material properties into the prediction equation would most likely improve our model as well.

The best model for bone strain prediction included impact force and cross-sectional area ($R^2=0.94$). These two variables determined the average axial stress and corresponding axial strain within the bone making this an expected result. Following this was the model including computed impact force and cross-sectional area ($R^2=0.84$). It is interesting to note that even after the effects of impact mass on leg acceleration had been accounted for, a lower coefficient of determination was observed when compared with the impact force and cross-sectional area model. The measurement of leg acceleration is only an approximation of the "true" impact acceleration. The true impact acceleration represents the total system mass being accelerated by the impact force, and can be calculated by dividing impact force by the impact mass. The leg acceleration represents a local acceleration at the leg accelerometer mounting site. Any skin movement that takes place underneath the accelerometer mounting site can influence the accuracy of leg acceleration. Skin movement can result in an overestimation [28] or underestimation [30] of leg acceleration depending on the stiffness of mounting and hardness of impact surface [31]. The variability in leg acceleration due to skin movement artifact may account for the lower R^2 seen in the computed impact force model when compared with the impact force model.

Limitations of the present study must be considered for an accurate interpretation of the results. The first limitation of this study is that the strain gauge and leg accelerometer were only mounted to the anteriomedial surface of the distal tibia. As such, the relationships between bone strain, impact force, and leg acceleration observed during this study can only be generalized to this location. The second and perhaps most important limitation of this study was the lack of muscle activity. The tension applied to the tibialis anterior tendon was low (24.4 ± 3.1 N) and used only to insure foot flexion at contact. The work of Milgrom et al. [32] suggested that energy absorption provided by muscle activity during impact can reduce bone strain at the anteriomedial tibia. Therefore, if muscle activity were expected to change between conditions, it is unlikely that the regression coefficients developed from this study would explain a similar amount of variance in bone strain during an in vivo loading situation.

In conclusion, the results obtained from this study have implications for both clinicians and researchers wanting to use force platforms and accelerometers to estimate impact loading on the skeletal system. Although it is not recommended that the prediction equations developed herein be used to estimate bone strain in vivo, the strong relationship between bone strain, impact force, and computed impact force suggested that force platforms and leg accelerometers can be used for a surrogate measure of bone strain at the distal tibia. In a repeated measure design, in which the subject serves as their own control, an increase in impact force coincides with an increase in bone strain. This is also true for leg acceleration if the effective mass of the impact can be approximated. For case control designs aimed at examining loading differences between two separate groups, external transducers by themselves should not be used for a surrogate measure of bone strain. Due to group differences in bone geometry, a difference in impact force or leg acceleration does not necessarily equate to a difference in bone strain. In this circumstance it is necessary to account for the tibial cross-sectional area. A normalization of the external transducer measurement to the tibial cross-sectional area should suffice if the primary mode of loading is due to axial compression.

Acknowledgment

The authors thank Dr. Philip M. Dixon for his help with the statistical analysis.

References

[1] Derrick, T. R., Hamill, J., and Caldwell, G. E., 1998, "Energy Absorption of Impacts During Running at Various Stride Lengths," Med. Sci. Sports Exercise, **30**, pp. 998–1002.

[2] Rubin, C. T., and Lanyon, L. E., 1985, "Regulation of Bone Mass by Mechanical Strain Magnitude," Calcif. Tissue Int., **37**, pp. 411–417.

[3] Turner, C. H., Forwood, M. R., Rho, J. Y., and Yoshikawa, T., 1994, "Mechanical Loading Thresholds for Lamellar and Woven Bone Formation," J. Bone Miner. Res., **9**, pp. 87–97.

[4] Owan, I., Burr, D., Turner, C. H., Qiu, J., Tu, Y., Onyia, J. E., and Duncan, R. L., 1997, "Mechanotransduction in Bone: Osteoblasts Are More Responsive to Fluid Forces Than Mechanical Strain," Am. J. Physiol., **273**, pp. C810–C815.

[5] Fehling, P. C., Alekel, L., Clasey, J., Rector, A., and Stillman, R. J., 1995, "A Comparison of Bone Mineral Densities Among Female Athletes in Impact Loading and Active Loading Sports," Bone, **17**, pp. 205–210.

[6] Daly, R. M., Rich, P. A., Klein, R., and Bass, S., 1999, "Effects of High-Impact Exercise on Ultrasonic and Biochemical Indices of Skeletal Status: A Prospective Study in Young Male Gymnasts," J. Bone Miner. Res., **14**, pp. 1222–1230.

[7] Pettersson, U., Nordström, P., Alfredson, H., Henriksson-Larsén, K., and Lorentzon, R., 2000, "Effect of High Impact Activity on Bone Mass and Size in Adolescent Females: A Comparative Study Between Two Different Types of Sports," Calcif. Tissue Int., **67**, pp. 207–214.

[8] Arendt, E., Agel, J., Heikes, C., and Griffiths, H., 2003, "Stress Injuries to Bone in College Athletes: A Retrospective Review of Experience at a Single Institution," Am. J. Sports Med., **31**, pp. 959–968.

[9] Hame, S. L., LaFemina, J. M., McAllister, D. R., Schaadt, G. W., and Dorey, F. J., 2004, "Fractures in the Collegiate Athlete," Am. J. Sports Med., **32**, pp. 446–451.

[10] Lanyon, L. E., Hampson, W. G. J., Goodship, A. E., and Shah, J. S., 1975, "Bone Deformation Recorded *In Vivo* From Strain Gauges Attached to the Human Tibial Shaft," Acta Orthop. Scand., **46**, pp. 256–268.

[11] Fyhrie, D. P., Milgrom, C., Hoshaw, S. J., Simkin, A., Dar, S., Drumb, D., and Burr, D. B., 1998, "Effect of Fatiguing Exercise on Longitudinal Bone Strain as Related to Stress Fracture in Humans," Ann. Biomed. Eng., **26**, pp. 660–665.

[12] Milgrom, C., Finestaon, A., Segev, S., Olin, C., Arndt, T., and Ekenman, I., 2003, "Are Overground or Treadmill Runners More Likely to Sustain Tibial Stress Fracture," Br. J. Sports Med., **37**, pp. 160–163.

[13] Whalen, R. T., Carter, D. R., and Steele, C. R., 1988, "Influence of Physical Activity on the Regulation of Bone Density," J. Biomech., **21**, pp. 825–837.

[14] Crossley, K., Bennell, K. L., Wrigley, T., and Oakes, B. W., 1999, "Ground Reaction Forces, Bone Characteristics, and Tibial Stress Fracture in Male Runners," Med. Sci. Sports Exercise, **31**, pp. 1088–1093.

[15] Hreljac, A., Marshall, R. N., and Hume, P. A., 2000, "Evaluation of Lower Extremity Overuse Injury Potential in Runners," Med. Sci. Sports Exercise, **32**, pp. 1635–1641.

[16] Ferber, R., McClay-Davis, I., Hamill, J., Pollard, C. D., and McKeown, K. A., 2002, "Kinetic Variables in Subjects With Previous Lower Extremity Stress Fractures," Med. Sci. Sports Exercise, **34**, p. S5.

[17] Bennell, K., Crossley, K., Jayarajan, J., Walton, E., Warden, S., Kiss, Z. S., and Wrigley, T., 2004, "Ground Reaction Forces and Bone Parameters in Females With Tibial Stress Fracture," Med. Sci. Sports Exercise, **36**, pp. 397–404.

[18] Valiant, G. A., 1989, "Transmission and Attenuation of Heel Strike Accelerations," *The Biomechanics of Distance Running*, P. R. Cavanagh, ed., Human Kinetics, Champaign, IL, pp. 225–247.

[19] Milner, C. E., Ferber, R., Pollard, C. D., Hamill, J., and Davis, I. S., 2006, "Biomechanical Factors Associated With Tibial Stress Fracture in Female Runners," Med. Sci. Sports Exercise, **38**, pp. 323–328.

[20] Milner, C. E., Hamill, J., and Davis, I., 2007, "Are Knee Mechanics During Early Stance Related to Tibial Stress Fracture in Runners?" Clin. Biomech. (Bristol, Avon), **22**, pp. 697–703.

[21] Zifchock, R. A., Davis, I., and Hamill, J., 2006, "Kinetic Asymmetry in Female Runners With and Without Retrospective Tibial Stress Fractures," J. Biomech., **39**, pp. 2792–2797.

[22] Denoth, J., 1986, "Load on the Locomotor System and Modeling," *Biomechanics of Running Shoes*, B. M. Nigg, ed., Human Kinetics, Champaign, IL, pp. 63–116.

[23] Derrick, T. R., 2004, "The Effects of Knee Contact Angle on Impact Forces and Accelerations," Med. Sci. Sports Exercise, **36**, pp. 832–837.

[24] Carter, D., 1978, "Anisotropic Analysis of Strain Rosette Information From Cortical Bone," J. Biomech., **11**, pp. 199–202.

[25] Nigg, B. M., 1986, "Biomechanical Aspects of Running," *Biomechanics of Running Shoes*, B. M. Nigg, ed., Human Kinetics, Champaign, IL, pp. 1–25.

[26] Shorten, M. R., and Winslow, D. S., 1992, "Spectral Analysis of Impact Shock During Running," International Journal of Sport Biomechanics, **8**, pp. 288–304.

[27] Gross, T. S., and Nelson, R. C., 1988, "The Shock Attenuation Role of the Ankle During Landing From a Vertical Jump," Med. Sci. Sports Exercise, **20**, pp. 506–514.

[28] Lafortune, M. A., Hennig, E. M., and Valiant, G. A., 1995, "Tibial Shock Measured With Bone and Skin Mounted Transducers," J. Biomech., **28**, pp. 989–993.

[29] Mercer, J. A., Vance, J., Hreljac, A., and Hamill, J., 2002, "Relationship Between Shock Attenuation and Stride Length During Running at Different Velocities," Eur. J. Appl. Physiol., **87**, pp. 403–408.
[30] Nsiah, B., Edwards, W. B., Meardon, S., Ward, E., and Derrick, T. R., 2006, "Spectral Analysis of Impact Accelerations Using Bone Versus Surface Mounted Accelerometers," Med. Sci. Sports Exercise, **38**, p. S267.
[31] Nigg, B. M., 1994, "Measuring Techniques," *Biomechanics of the Musculo-Skeletal System*, B. M. Nigg and W. Herzog, eds., Wiley, New York, NY, pp. 199–364.
[32] Milgrom, C., Finestone, A., Levi, Y., Simkin, A., Ekenman, I., Mendelson, S., Millgram, M., Nyska, M., Benjuya, N., and Burr, D., 2000, "Do High Impact Exercises Produce Higher Tibial Strains Than Running?" Br. J. Sports Med., **34**, pp. 195–199.